Chapter 1 | Introduction and Literature

1.1 INTRODUCTION

The history of additive manufacturing (AM) dates back to the year 1980 when the first 3D printer was invented by Chuck Hull. A process called `Stereolithography' was developed, which used a laser to cure a liquid photopolymer layer-by-layer, resulting in a solid object [1]. Over the years, AM technology has advanced significantly, with new materials, processes and applications being developed. Today, additive manufacturing is used in many industries which produce aerospace, automotive, health care and consumer goods. As the technology continues to advance, it has the potential to transform manufacturing even further, with the usage of new materials, faster printing speeds and larger build volumes [2].

The definition of Additive Manufacturing as per ISO/ASTM 52900 [3] is as follows:

"A process of joining materials to make objects from 3D model data, usually layer upon layer, as opposed to subtractive manufacturing methodologies."

1.2 ADDITIVE MANUFACTURING OVER SUBTRACTIVE MANUFACTURING

Additive manufacturing builds up an object layer by layer using CAD models whereas subtractive manufacturing starts with a larger slice of material and removes material until the final product is achieved. In additive manufacturing, the process starts with a digital model of the object that is to be produced. This model is sliced into layers and the printer then adds material one layer at a time until the object is complete. In contrast, subtractive manufacturing starts with a block of material, such as metal or plastic, and removes the material until the final product is achieved. This is done through processes like milling, turning and drilling, where a cutting tool is used to remove material from the workpiece. The difference is shown in the pictorial view in Fig.1.1.

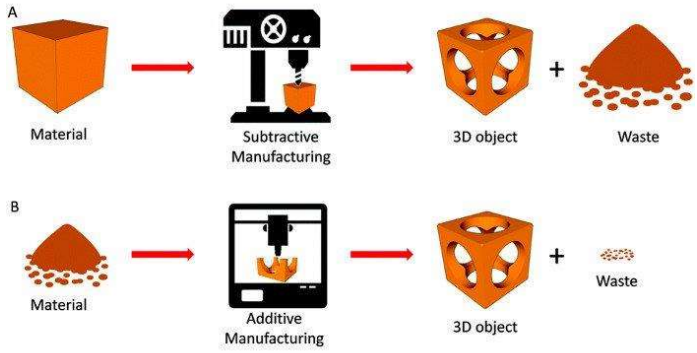

Fig.1.1 Process comparison of additive manufacturing and subtractive manufacturing [4].

Additive manufacturing offers several advantages over subtractive manufacturing. First, it allows for the creation of complex shapes and geometries that would be difficult or impossible to produce using subtractive manufacturing techniques. Second, it generates less waste since only the necessary amount of material is used, while subtractive manufacturing often results in significant material wastage. Third, additive manufacturing offers faster production times since it does not require the same level of tooling and setup that subtractive manufacturing requires. Finally, additive manufacturing allows greater customization and flexibility, making it ideal for small-scale production [5].

1.3 CLASSIFICATION OF ADDITIVE MANUFACTURING TECHNOLOGIES

Additive manufacturing technologies can be classified into seven main categories [6]:

1.3.1 Powder Bed Fusion (PBF)

Powder bed fusion (PBF) is an additive manufacturing technique that uses a high-powered energy source such as a laser or an electron beam to selectively fuse or melt successive layers of metallic or non-metallic powders to build up complex three-dimensional objects. It is represented in Fig.1.2. PBF is suitable for producing complex metal parts with high accuracy and good mechanical properties. It can be used for metals

and alloys such as titanium, aluminium, stainless steels and other advanced alloys. However, PBF has limitations such as slow processing speed, high equipment cost and limited part size.

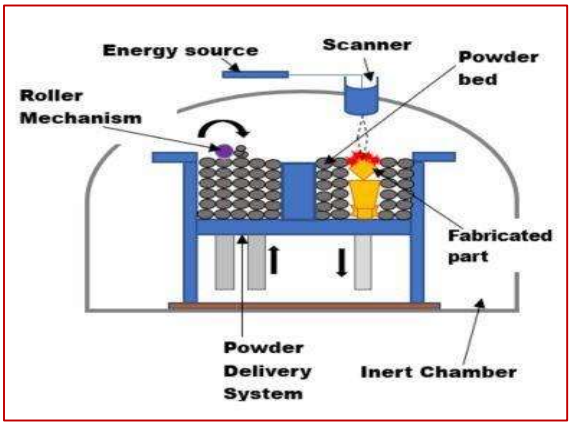

Fig. 1.2 Schematic diagram for Powder bed fusion PBF/SLM [7].

Selective Laser Melting (SLM)

Selective laser melting (SLM) is a type of PBF technique that uses a high-powered laser to selectively melt metal powder particles to form complex 3D objects. In SLM, the powder is first spread uniformly over the build platform. The laser then scans the powder bed and selectively melts the metal powder particles in accordance with the 3D design model. After each layer is melted, the build platform moves down by a layer thickness, and a new layer of powder is spread over the previous one. The process is repeated until the final object is formed. The process parameters in selective laser melting (SLM) are crucial for achieving the desired mechanical properties, surface finish and dimensional accuracy of the final parts. Three important process parameters in SLM are laser power, scan speed and layer thickness. Optimal settings of these parameters can result in improved part quality and productivity [8].

1.3.2 Direct energy deposition (DED)

Direct Energy Deposition (DED) is an additive manufacturing process that entails melting and fusing materials with a laser or an electron beam as the focused energy source. The technique permits the construction of intricate geometries and used for materials such as metals, ceramics and polymers. Aerospace, automotive and medical industries frequently use DED for rapid prototyping, repair and production of high-performance components [9]. The DED is presented in Fig. 1.3.

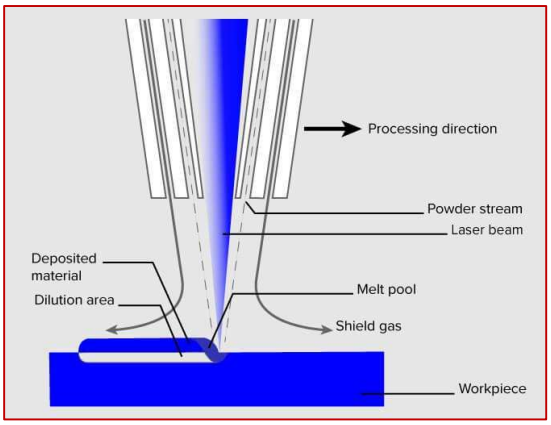

Fig. 1.3 Schematic diagram for Direct Energy Deposition (DED) [9].

1.3.3 Material Extrusion (ME)

Material extrusion is a method of additive manufacturing in which a material is extruded through a nozzle to produce a three-dimensional object. Fused filament fabrication (FFF) or fused deposition modelling (FDM) are common names for this process. It is a popular and extensively utilized technique for producing prototypes, models and small production parts. The material used can be plastic, metal or even food [10]. The ME technique is presented in Fig. 1.4.

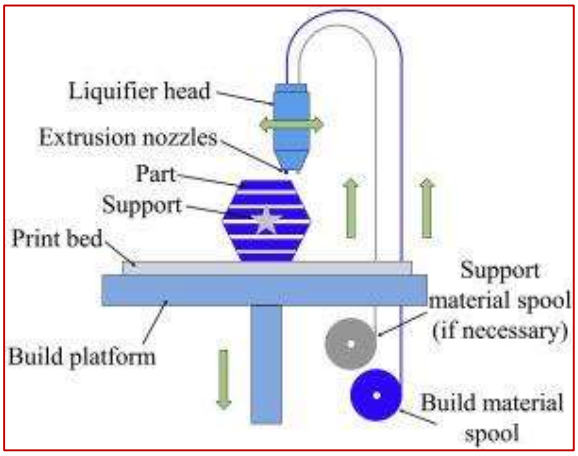

Fig. 1.4 Schematic diagram for Material Extrusion (ME) [10].

1.3.4 Sheet lamination (SL)

Sheet lamination (SL) is an additive manufacturing process that creates three-dimensional objects by layering and adhering thin sheets of substance, such as paper or plastic. Typically, the sheets are cut into the desired shape using a computer-controlled laser or knife, and then they are bonded together using heat, pressure, or adhesive. SL is a relatively inexpensive and versatile additive manufacturing technique that is ideally adapted for producing large, lightweight objects with intricate geometries [11]. The SL technique is presented in Fig. 1.5.

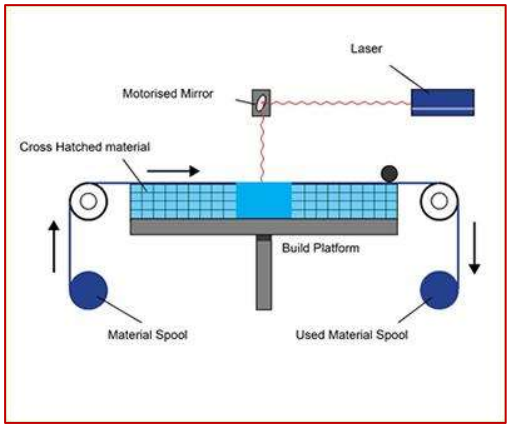

Fig. 1.5 Schematic diagram for Sheet Lamination (SL) [11].

1.3.5 Binder jetting (BJ)

Binder jetting is an additive manufacturing process that entails depositing layers of powdered material and adhering them with a liquid binder. This procedure generates a three-dimensional object that can be sintered or cured to attain its ultimate form. Binder jetting is frequently used in the manufacturing of metal or ceramic components and is renowned for its speed and efficiency [12]. The BJ technique is presented in Fig. 1.6.

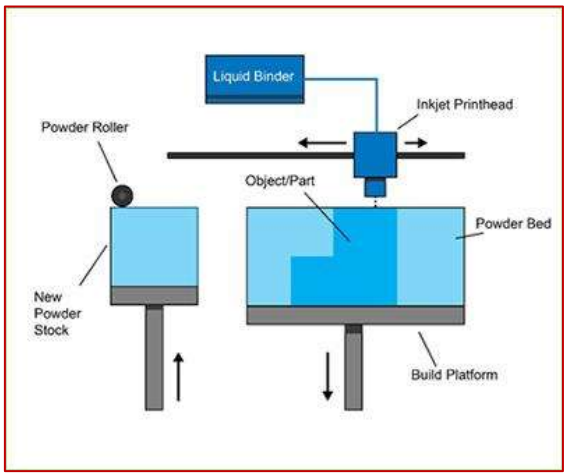

Fig. 1.6 Schematic diagram for Binder Jetting [12].

1.3.6 Vat Photopolymerization (VP)

Vat photopolymerization (VP) is a 3D printing method that employs a photopolymer substance in liquid form. The resin is cured layer by layer using a UV laser or projector as the light source. It may be necessary to use supports to hold up overhanging parts until they have completely cured [13]. The VP technique is presented in Fig. 1.7.

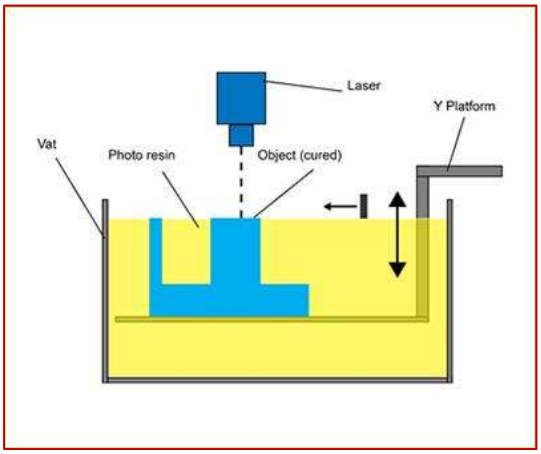

Fig. 1.7 Schematic diagram for Vat Photopolymerization [13].

1.3.7 Material Jetting (MJ)

Material jetting (MJ) is a 3D printing process in which liquid photopolymers are selectively jetted onto a construction platform and cured using ultraviolet light. This procedure produces intricate, high-resolution components with smooth surface finishes. This technology is frequently employed in the production of prototypes, models and limited production quantities [14]. The MJ technique is presented in Fig. 1.8.

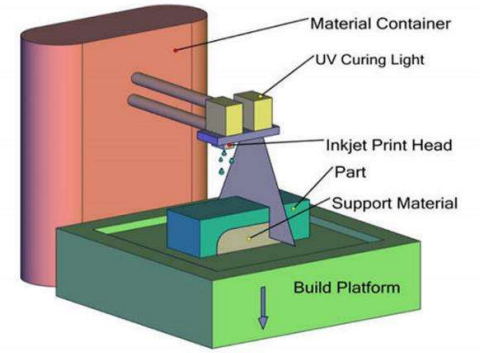

Fig. 1.8 Schematic diagram for Material Jetting [14].

1.4 Important Factors in PBF-LB/SLM

1.4 .1 Process Parameters

The process parameters in selective laser melting are laser power (P, in watt), scan speed (v, in mm/s), layer thickness (t, in mm), hatch spacing (h, in mm) and energy density (E,

in J/mm^3). These are interdependent and can be related through a formula that governs the energy density and dimensions of melt pool.

The formula for the energy density (E) can be expressed as [15]:

$$E = \frac{P}{v \times h \times t} \quad \text{(Eq.1.1)}$$

The formula for the melt pool width (w, in mm) can be expressed as [16]:

$$W = \frac{2.1 \times \sqrt{P}}{v \times t} \quad \text{(Eq. 1.2)}$$

The above formula indicates that increasing the laser power or decreasing the scan speed or layer thickness can result in a wider melt pool, which can affect the part quality by influencing the microstructure, porosity and residual stresses.

For achieving the best quality of the product, process parameters need to be optimized. There are several methods for optimizing process parameters in selective laser melting (SLM). One common approach is the Design of Experiments (DOE), which involves systematically varying the process parameters and analyzing the resulting part quality to determine the optimal parameter settings.

In a study by Khorasani et al. (2020) [17], DOE was used to optimize the process parameters in SLM of Ti-6Al-4V alloy. Laser power, scan speed, layer thickness and laser spot diameter were varied and the resulting part density and surface roughness were measured. Based on the DOE results, the optimal process parameters for achieving the desired part quality were determined. Experiments were conducted at the optimal parameter settings and it was realized that the resulting part quality was improved compared to quality obtained with the initial parameter settings.

1.4.2 Defects in Powder bed fusion

In Powder Bed Fusion (PBF) using Laser Beam, defects can be generated due to various reasons. Some of the common defects that can occur during PBF using Laser Beam are given below [18]:

Lack of Fusion: Lack of fusion is a defect that occurs when the laser does not properly melt the powder particles and fuse them together. This can be caused by insufficient laser power, improper focus or incorrect scan speed.

Balling: Balling is another important defect that occurs when small balls of molten metal are formed on the surface of the part being printed. It can be caused by excessive laser power, insufficient powder spreading or incorrect scan strategy.

Porosity: Porosity is a defect that occurs when gas pockets are trapped inside the part during the printing process. Several factors such as insufficient laser power, improper powder density or incorrect scan strategy are responsible for porosity.

Warping: Warping is a defect that occurs when the printed part undergoes significant distortion during the printing process. This can be caused by thermal stresses induced during printing, improper support structure design or inadequate cooling.

Cracking: Cracking is a defect that occurs when the part experiences significant thermal stresses during printing, which can cause the material to crack. Several factors, including excessive laser power, improper support structure design or inadequate cooling are responsible for the cracking.

Inconsistent Material Properties: Inconsistent material properties can be obtained when the powder bed is not properly mixed or has varying particle sizes. It can result in

inconsistent melting and solidification rates, which can affect the material properties of the final part.

These defects can have a significant impact on the mechanical properties and overall quality of the printed parts and therefore, it is important to understand the causes and mechanisms of these defects in order to optimize the printing process and improve the quality of the printed parts.

1.4.3 Materials for PBF-LB/SLM

Some of the common metals and alloys used in SLM include titanium, stainless steels, aluminum, copper and nickel alloys. The choice of metal depends on the specific application and requirements of the part, such as strength, tribological properties such as wear resistance and corrosion resistance [19].

Titanium and its alloys are popular choice for SLM due to high strength-to-weight ratio, biocompatibility and corrosion resistance. These are often used in aerospace, medical and dental applications. However, titanium can be difficult to print due to its high melting point, which requires a high-powered laser and precise control of the SLM process [20].

Stainless steels constitute another commonly used alloy group for SLM due to their high strength, corrosion resistance and versatility. They are extensively used in automotive, aerospace and industrial applications. Stainless steels can be printed with relatively low laser power, which makes it easier to print compared to the printing of titanium alloys.

Aluminum alloys are also used in SLM due to low density, high thermal conductivity and excellent strength-to-weight ratio. They are widely used in aerospace, automotive and consumer products. However, aluminum is difficult to print due to its high reflectivity, which requires special laser parameters and preparation of powders.

Copper and nickel alloys are used in SLM for their high electrical conductivity, thermal conductivity and corrosion resistance. They are often used in electronic and industrial applications. Copper and nickel alloys can be printed with high laser power, which allows for rapid printing and high-density parts.

To determine suitability of a given metal for SLM, it is important to consider factors such as melting temperature, powder size and shape, compatibility with SLM process, mechanical properties and cost [21]. In addition, the quality and composition of the SLM part can be assessed using analytical techniques such as SEM, XRD, and EDX. These techniques can provide information on the microstructure, composition and defects of the SLM part, which can be used to assess its quality and suitability for the intended applications [22].

1.4.4 Recent developments

There are ongoing developments in materials suitable for SLM to improve the mechanical properties, printability and functionality of SLM parts.

One recent development is the use of high-entropy alloys (HEAs) for SLM [23]. HEAs are a new class of alloys composed of five or more metallic elements in equimolar or near-equimolar ratios. HEAs have attracted attention for their excellent mechanical properties, such as high strength, hardness and ductility. Researchers have recently demonstrated the feasibility of printing HEAs using SLM, which opened up new opportunities for developing advanced materials with tailored properties. Another recent development is the use of functionally graded materials (FGMs) for SLM [24]. FGMs are composite materials with graded composition and microstructure that vary gradually from one end of the part to the other. FGMs can provide tailored properties, such as stiffness, thermal expansion, and electrical conductivity to meet specific requirements of

the part. Researchers have explored the use of SLM for printing FGMs with different compositions and microstructures. In addition, researchers have explored the use of SLM for printing metallic glasses, which are amorphous materials with disordered atomic structures that exhibit unique mechanical, physical and chemical properties [25]. Metallic glasses have attracted attention for their high strength, corrosion resistance and wear resistance.

Finally, nanostructured metals have been explored for use in SLM. Nanostructured metals are metals with a grain size of less than 100 nm. Nanostructured metals exhibit improved mechanical properties such as high strength, ductility and fatigue resistance, compared to the properties of conventional metals. Researchers have explored the use of SLM for printing nanostructured metals, which offers new opportunities for developing advanced materials with enhanced properties [26]. These are just a few examples of recent developments in materials suitable for SLM. As the technology continues to evolve, it is likely that new materials with tailored properties will be developed and used in various applications.

1.4.5 Powder Specifications for SLM

Powder characteristics play a critical role in the success of Selective Laser Melting (SLM). The powder must meet certain specifications to achieve optimal performance and part quality. The required powder specifications for SLM include particle size distribution, morphology, flowability and chemical composition. Particle size distribution is an important powder characteristic that affects the flowability, packing density and surface roughness of the printed parts. The ideal particle size distribution for SLM depends on the laser beam size and the layer thickness. Typically, the powder particle size should be in the range of 10 to 50 microns, with a narrow size distribution. Morphology is another important powder characteristic that affects the flowability and

packing density of the powder. The powder particles should be spherical and have a smooth surface to ensure uniform packing and minimum porosity in the printed parts. Non-spherical particles or particles with rough surfaces can cause uneven packing and lead to defects in the printed parts. Flowability is a critical powder characteristic that affects the ability of the powder to flow smoothly and uniformly in the build chamber [27]. The powder should have good flowability to ensure uniform packing and minimize the risk of powder caking or clumping. The flowability of the powder can be measured by using various techniques, such as the Hall flow meter or the Carr index. Chemical composition is an important powder characteristic that affects the properties and performance of the printed parts. The powder should have a uniform chemical composition and purity to ensure consistent part quality and mechanical properties. The chemical composition of the powder can be measured by using various techniques, such as X-ray fluorescence spectroscopy or atomic absorption spectroscopy. In summary, the required powder specifications for SLM include particle size distribution, morphology, flowability, and chemical composition. These powder characteristics play a critical role in the success of SLM and the quality of the printed parts.

1.5 NEED FOR PROCESSING OF STEELS BY ADDITIVE MANUFACTURING

The development and processing of steels using Selective Laser Melting (SLM) have gained significant attention in recent years due to the unique capabilities of SLM in fabricating complex and functional metal parts. The ability to produce near-net-shape parts with excellent mechanical properties and high precision has made SLM an attractive technology for producing high-performance steel parts. One of the key advantages of SLM for steel processing is the ability to produce fully dense parts with low porosity, which leads to superior mechanical properties [28]. SLM can produce complex geometries that are difficult to achieve using traditional manufacturing processes, such

as casting or forging. The process also enables the production of graded structures, where the composition and microstructure can be varied spatially to optimize the mechanical properties of the part. Another advantage of SLM for steel processing is the ability to use high-strength, high-alloy steels that are difficult to process using traditional manufacturing methods. These materials often have low ductility and are prone to crack during casting or forging. SLM can overcome these limitations by using fine powder that is melted layer-by-layer, allowing for precise control over the microstructure and mechanical properties of the part [29]. The development of new steels specifically for SLM is also an area of active research. These alloys can be designed to take advantage of the unique capabilities of SLM, such as the ability to produce complex geometries and graded structures. For example, a recent study developed a new steel that combines high strength and ductility by controlling the composition and microstructure of the material during SLM processing [30].

1.6 IMPORTANCE OF MARAGING STEEL IN AM

Maraging steel is a popular choice in additive manufacturing (AM) due to its unique combination of properties such as high strength, toughness and ductility. The high strength of maraging steel is attributed to precipitation hardening, which involves the formation of intermetallic compounds during heat treatment [31]. Moreover, maraging steel has excellent compatibility with AM processes such as laser powder bed fusion (LPBF) and electron beam melting (EBM) due to its low carbon content and low thermal conductivity. These properties enable maraging steel to be processed with high energy density and achieve high-quality parts with minimal distortion [32]. There is also a growing demand for maraging steel in various industries such as aerospace, automotive and medical devices, which are among the key drivers of AM adoption. A recent study by M Skrzyniarz et al. (2022) [33] investigated the suitability of maraging steel for AM

applications and concluded that maraging steel is an excellent material for AM due to its unique combination of properties and compatibility with AM processes.

1.7 MARAGING STEELS

Maraging steels are high-strength steels, characterized by very low carbon content and contain substitutional elements such as cobalt, molybdenum and titanium to provide age-hardening. The name "maraging" was derived from martensite and aging. Decker, Eash, and Goldman discovered in 1960 that cobalt and molybdenum can effectively harden Fe-Ni martensites [34]. Based on this proposition, a variety of alloy compositions have been produced. As shown in Table. 1.1, Alloy A, the 25% nickel steel, is a semi-austenitic composition; that is, after solution-annealing, M_s temperature is sufficiently low for the alloy to remain austenitic upon cooling to room temperature. The 20% nickel steel, Alloy B, has a M_s temperature of the order of 200^oC and completely transforms to martensite after solution-annealing. In this case, hardening requires only a maraging heat treatment in the 425-485^oC temperature range. The alloys C, D, and E correspond to the maraging steel grades 18Ni (200), 18Ni (250), and 18 Ni (300). All of these alloys have 18% nickel as the base element with various amounts of cobalt, molybdenum and titanium to produce the required levels of strength. Titanium is used in these compositions as a supplemental hardener, but the primary strengthening effect comes from the combination of cobalt and molybdenum. Alloy F is a composition with greater resistance to austenite reversion which has proved to be of interest for elevated-temperature magnetic applications. Alloy G is a recent composition that achieves a 2400 MPa strength level. Alloy H is a cast alloy. Alloy I is the so-called 12-5-3 maraging steel. In all the alloys, the carbon content is specified as 0.03 wt % maximum. Titanium in most cases, plays a double role of hardening as well as refining agent to tie up the residual carbon.

Table 1.1 Nominal chemical composition of maraging steels in wt% [35].

Alloy	Ni	Co	Mo	Al	Ti	Other	Fe
A	25	-	-	0.3	1.4	0.4 Nb	Bal
B	20	-	-	0.3	1.4	0.4 Nb	Bal
C	18	8	3.2	0.1	0.2	-	Bal
D	18	8	5.0	0.1	0.4	-	Bal
E	**18**	**9**	**5.0**	**0.1**	**0.6**	**-**	**Bal**
F	15	9	5.0	0.7	0.7	-	Bal
G	18	12	4.0	0.1	1.6	-	Bal
H	17	10	4.6	0.1	0.3	-	Bal
I	12	-	3.0	0.3	0.2	5 Cr	Bal

Typically, these steels are solution-annealed at 815ºC for 1 hour, although other annealing temperatures or multiple annealing heat-treatments are used in certain cases. After annealing, the alloys transform completely to martensite upon cooling to room temperature. Because of the high nickel content and the virtual absence of carbon, hardenability is not a problem and the cooling rate after annealing is not important. In the as-annealed condition, the alloys have hardness of the order of Rockwell C30 and can be readily machined or fabricated. Hardening is then achieved by maraging, generally using an aging treatment at (480-500) °C for (3-5 hours) [36]. Dimensional changes during age-hardening are very small and completely finished pieces can be machined in the annealed condition and then hardened by maraging. The alloys are readily weldable and possess resistance to hydrogen embrittlement and stress-corrosion cracking and generally exhibit superior properties over high-strength low-alloy steels. Several basic characteristics of maraging steels are directly related to the characteristics of the iron-rich end of the iron-nickel phase diagram, as shown in Fig.1.9(a), given by Owen and Liu.s [37]. It can be seen that upon cooling, an alloy containing, say, 18% nickel from the austenite field, the austenite will not decompose into the equilibrium austenite and ferrite, even if held for very long times in the two-phase region. Instead with further cooling, the austenite transforms to martensite that has a *bcc* crystal structure.

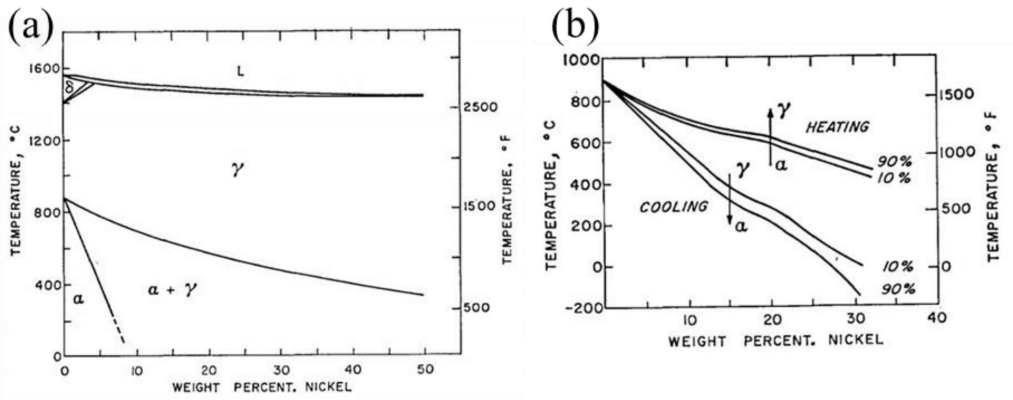

Fig.1.9 (a) Iron-nickel phase diagram (b) Metastable martensite phase transformation [38].

The martensite transformation temperatures as a function of nickel content are shown in the metastable equilibrium diagram of Jones and Pumphrey in Fig.1.9(b). Comparing this diagram (Fig. 1.9 b) to the equilibrium diagram in Fig. 1.9 (a), one can see that, upon cooling, the beginning of the gamma-to-alpha transformation occurs at relatively low temperatures. Similarly, the end of transformation is accelerated. Consequently, the duplex alpha-gamma phase field is severely suppressed, which favors the complete transformation of gamma (austenite) upon cooling.

1.7.1 Effect of alloying elements

The addition of alloying elements to 18Ni300 maraging steel helps to improve its mechanical properties by forming stable precipitates and intermetallic compounds that contribute to its strength, hardness and toughness [39]. The resulting microstructure is more homogeneous and resistant to wear, corrosion and fatigue, making maraging steel a popular choice for high-strength applications in aerospace, defense and tooling industries.

Cobalt (Co): Cobalt is added to maraging steel in order to increase its strength, toughness, resistance to wear and corrosion. It forms carbides and intermetallic compounds with other elements in the steel, which contribute to its strength and hardness.

Cobalt also promotes the formation of fine and uniform precipitates during the aging process and contributes to homogeneous microstructure and improved mechanical properties.

Molybdenum (Mo): Molybdenum is added to maraging steel to enhance its high-temperature strength and hardness. It forms carbides and intermetallic compounds that are stable at high temperatures, which helps to maintain the mechanical properties at elevated temperatures. Molybdenum also improves resistance to corrosion and wear.

Titanium (Ti): Titanium is added to maraging steel to improve its strength, toughness and resistance to corrosion and oxidation. It forms titanium carbides and intermetallic compounds with other elements in the steel, which contribute to its strength and hardness. Titanium also promotes the formation of fine and uniform precipitates during the aging process, which results in homogeneous microstructure and improved mechanical properties.

Aluminum (Al): Aluminum is added to maraging steel to improve its strength, toughness, resistance to corrosion and wear. It forms aluminum carbides and intermetallic compounds with other elements in the steel, which contribute to its strength and hardness. Aluminum also promotes the formation of fine and uniform precipitates during the aging process which cause improvement in mechanical properties.

Nickel (Ni): Nickel in maraging steel offers several advantages, including the formation of intermetallic compounds such as Ni_3Mo and Ni_3Ti, which contributes to the high strength and durability. Additionally, nickel improves the corrosion resistance and weldability of steel. In addition, nickel reduces the rate of ageing, or the loss of ductility that maraging steels experience over time.

Carbon (C): Carbon is a crucial element of maraging steels, as it promotes the formation of intermetallic compounds that give the steel its strength and hardness. Compared to other elements, the carbon content is relatively low (0.03 wt%), but it is still a significant contributor to the strength and durability of the steel.

Iron (Fe): Iron in 18Ni300 maraging steel strikes a balance between durability and strength. The majority of the steel is composed of iron, which creates a solid solution with nickel. The iron-nickel solid solution contributes to the steel's high strength while preserving its ductility and tensile strength.

1.7.2 Precipitation behaviour of maraging steel

Maraging steel is a high-strength steel that is known for its exceptional strength, toughness and resistance to corrosion. It is primarily composed of iron, nickel, and cobalt along with other alloying elements in various grades. High strength is achieved from precipitation hardening that involves the formation of small and uniform precipitates within the steel matrix that impede the movement of dislocations, resulting in increase in strength [40].

During the precipitation hardening process, the maraging steel is heated to an elevated temperature and held for a certain period of time to allow the alloying elements to diffuse and form small, uniform precipitates of intermetallic compounds. These precipitates are typically much smaller and are evenly distributed throughout the matrix. The formation of these intermetallic precipitates has a significant influence on the properties of the steel. First, the presence of these particles impedes the movement of dislocations, or defects, in the crystal structure of the steel. This makes it more difficult for the steel to deform, leading to an increase in strength and hardness. Second, the precipitates can also trap and immobilize impurities, such as carbon and oxygen, which would otherwise weaken the

steel. This enhances the toughness and resistance to corrosion. The specific type and size of the precipitates formed in maraging steel depend on various factors, including the composition of the steel, the processing temperature, time and the cooling rate. By carefully controlling these parameters, it is possible to tailor the properties of the steel to specific applications, such as aerospace, defense and industrial applications where high strength and toughness are required [41]. There are several types of precipitates that can be formed in maraging steel, including Ni_3Mo, Ni_3Ti, and Ni_3Al. These intermetallic compounds have different crystal structures and chemical compositions, which affect their properties and consequent behaviour in various applications [42].

Ni_3Mo precipitates are typically formed in maraging steel after aging at a temperature of around 500-550°C for several hours. These precipitates have a body-centered cubic (*bcc*) crystal structure and can contribute to high strength and toughness. These precipitates also provide resistant to deformation as they act as obstacles to dislocation movement in maraging steels at high temperatures [43].

Ni_3Ti precipitates are formed by aging maraging steel at a temperature of around 450-500°C for several hours. These precipitates have a face-centered cubic (*fcc*) crystal structure and are known for imparting high strength and hardness. They are, however, relatively brittle, which make them more susceptible to fracture under certain conditions [44].

Ni_3Al precipitates are formed by aging maraging steel at a temperature of around 600-650°C for several hours. These precipitates have a hexagonal close-packed (*hcp*) crystal structure and are known to contribute high strength, toughness and corrosion resistance. These precipitates also provide strength at high temperatures as they restrict dislocation motion [45].

Fe_2Mo are formed by aging the steel at a temperature of around 520-575°C for several hours. Fe_2Mo precipitates have a body-centered cubic (*bcc*) crystal structure and are known for their high strength and toughness, similar to Ni_3Mo precipitates. Fe_2Mo precipitates are often used in combination with Ni_3Mo precipitates to further increase the strength and toughness of maraging steel. The precise role of Fe_2Mo precipitates in the precipitation behavior of maraging steel can depend on the specific alloy composition and processing conditions used [46].

1.7.3 Austenite reversion in maraging steel

Austenite reversion is a phenomenon that can occur during the aging of maraging steel. During the initial stages of aging, precipitation of intermetallic compounds takes place. As these precipitates grow and coarsen over time, the remaining austenite in the steel may begin to transform to martensite, a harder and more brittle phase of the steel. However, in some cases, the austenite may instead revert back to the original microstructure of the steel, known as the primary austenite phase. This is referred to as austenite reversion, and it is typically observed in maraging steels that have a relatively high content of nickel or other austenite-stabilizing elements. The exact mechanism of austenite reversion in maraging steel is not fully understood, but it is thought that a combination of diffusion of atoms and changes in the crystal structure of the steel are involved. During aging, the nickel atoms in the steel may diffuse out of the precipitates and into the remaining austenite, leading to a decrease in the concentration of austenite-stabilizing elements and an increase in the likelihood of martensitic transformation [47]. However, at high aging temperatures, some of the nickel may diffuse back into the precipitates, which can stabilize the remaining austenite and prevent further transformation. The effect of austenite reversion on the properties of maraging steel can be significant. If a significant amount of austenite reverts to the primary austenite phase,

the strength and toughness of the steel may be reduced, since the primary austenite phase is typically softer and less ductile than the martensitic phase. However, if the reversion is limited and the steel is processed carefully, austenite reversion can be used to enhance the toughness and ductility of the material, since the primary austenite phase is more ductile and less brittle than martensite [48].

1.8 APPLICATIONS OF ADDITIVE MANUFACTURED MARAGING STEELS

Maraging steels are widely used in the aerospace, defence and medical industries due to their high strength, toughness and corrosion resistance. The combination of AM and maraging steel has opened up new possibilities in product design and manufacturing [49]. Some current applications of additive manufactured maraging steels are mentioned below.

Aerospace and Defense Industry: Maraging steels are used in aerospace and defense applications such as rocket and missile components, aircraft landing gears and engine parts. Additive manufacturing of maraging steels can produce complex geometries with high strength, which can reduce weight and improve performance. NASA in 2015, has used AM to produce rocket engine parts made of maraging steel for its Space Launch System (SLS) program [50].

Medical Industry: Additive manufactured maraging steels are also used in medical implants, such as orthopedic implants, surgical tools and medical instruments [51].

Tooling and Molds: Additive manufactured maraging steels are used in tooling and molds for manufacturing processes such as injection molding and die casting. Maraging steels have high wear resistance and can withstand high temperatures, making them ideal for tooling and molds.

Automotive Industry: Maraging steels are used in the automotive industry for engine components and suspension systems due to its high strength and corrosion resistance. AM of maraging steels can reduce lead times and costs for producing complex parts with high performance.

Energy Industry: Maraging steels are used in the energy industry for oil and gas exploration and production. Additive manufacturing of maraging steel can produce components for drilling and extraction equipment that can withstand high pressures and corrosive environments [52].

1.9 RESEARCH INVESTIGATIONS ON AM MARAGING STEELS

1.9.1 TENSILE BEHAVIOUR

Characterization of microstructure and mechanical behaviour of metals and alloys processed by AM has received worldwide attention in the recent past. Studies on microstructure and mechanical behaviour of additive manufactured steels are mostly carried out in 316L austenitic stainless steels [53-56], 17-4 PH [57, 58] and 15-5 PH steels [59], tool steels [60] and some in maraging steels. Most of these studies are aimed at exploring the effect of process parameters and subsequent heat treatments on microstructure, texture, tensile properties and wear characteristics.

Tan et al.,[61] processed M300 maraging Steel (with 99.9 % density), using optimized process parameters by SLM. Microstructural evolution, nanoprecipitation behaviour and mechanical characteristics of SLM-manufactured M300 steel were investigated. The results indicated that the characteristics of 300M steel generated by SLM and subsequent solution and ageing heat treatments were comparable to those of conventional wrought steels as given in Table 1.2. As-fabricated samples revealed very fine grains (0.31μm) as shown in Fig. 1.10.

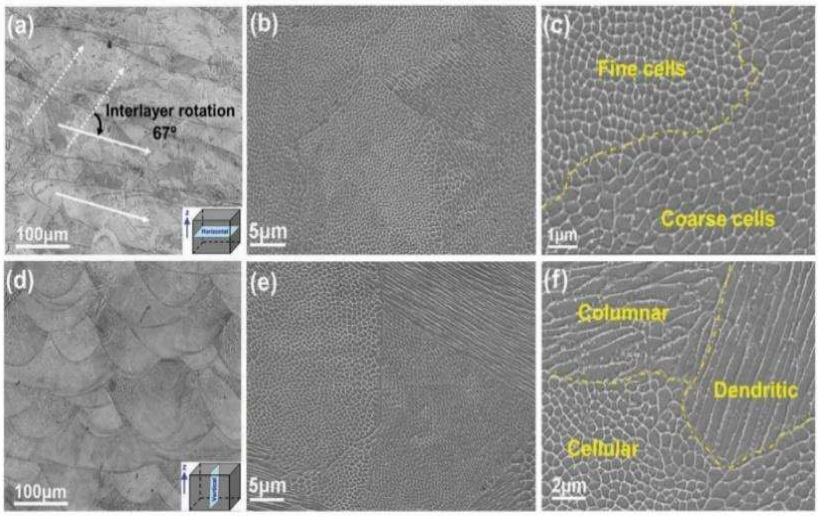

Fig.1.10 As fabricated microstructure (a) top face showing 67° inter layer rotations, (b, c) magnified view of 'a' showing fine and coarse cellular grains, (d) melt pool in transverse face and (e, f) magnified view showing mainly columnar grains.

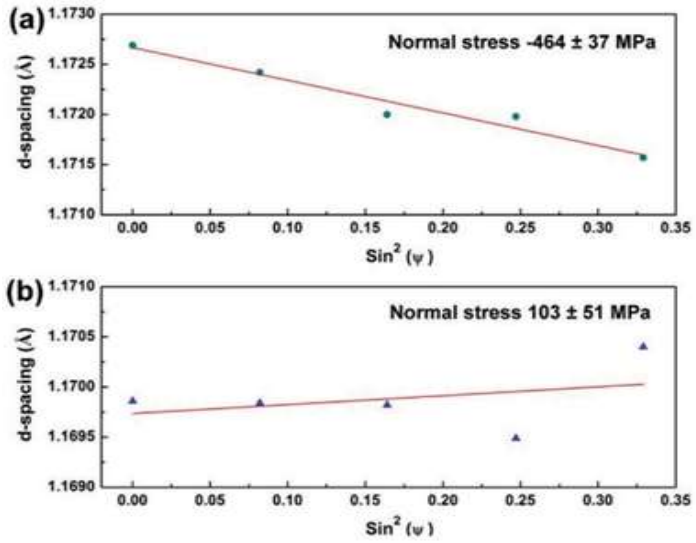

Fig. 1.11 Residual stresses in samples after: (a) as-fabrication (b) heat treatment.

Build layer-based anisotropy was also observed in as-fabricated and heat-treated samples, and after heat treatment, the strength improved and also residual stresses were relieved as indicated in Fig. 1.11. After aging, strength was improved at cost of ductility. Compared to horizontal samples, the hardness and tensile properties of the vertical sample were found to be comparatively lower.

Table 1.2 Mechanical properties of grade 300MS produced through Selective Laser Melting (SLM) and the conventional wrought route [61].

Layer Orientation	Samples	Ultiamte Tensile strength (MPa)	Yield Strength (MPa)	Elongation (%)	Hardness (HRC)
Horizontal	SLM as-fabricated	1165 ± 7	915 ± 7	12.4 ± 0.1	34.8 ± 0.2
	SLM aged	2014 ± 9	1967 ± 11	3.3 ± 0.1	54.6 ± 0.8
	SLM solution	1025 ± 5	962 ± 6	14.4 ± 0.4	29.8 ± 1.3
	SLM solution-aged	1943 ± 8	1882 ± 14	5.6 ± 0.1	53.5 ± 0.8
Vertical	SLM as-fabricated	1085 ± 19	920 ± 24	11.3 ± 0.3	35.7 ± 1.1
	SLM aged	1942 ± 31	1867 ± 22	2.8 ± 0.1	52.9 ± 1.2
	SLM solution	983 ± 13	923 ± 16	13.7 ± 0.7	27.5 ± 0.4
	SLM solution-aged	1898 ± 33	1818 ± 27	4.8 ± 0.2	51.3 ± 0.9
Standard	Wrought	1000–1170	760–895	6–15	35
	Wrought aged	1930–2050	1862-2000	5–7	52

Kempen et al., [62] investigated the effects of varying SLM processing parameters (such as layer thickness, scan speed, and hatch spacing) and age-hardening heat treatments on the mechanical characteristics and microstructure of 300M steel. The ultimate tensile strength (UTS) was found to be increased from 1290 MPa to 2216 MPa due to age hardening at 480°C for 5 hours. However, elongation was decreased from 13% to 2%. Due to the effect of heat treatment, Young's Modulus was found to be increased to a value of 189 GPa.

Casati et. al., [63] investigated the influence of ageing treatment on the mechanical properties of AM M300 steel. As built samples displayed cellular microstructure. Several laser tracks depicted the development of epitaxial grain growth. After solution treatment,

visible laser marks in the mesostructure were vanished and coarse martensite grains were developed by replacing the cellular structure. Aging significantly enhanced the tensile strength compared to that of the as-built condition, but decreased the ductility.

Yin et al., [64] investigated the impact of ageing treatments on the mechanical and tribological properties of SLM M300 steel. The ideal ageing treatment for SLM M300 steel (490°C for 3 hours) was found to be effective for enhanced wear resistance and tensile strength.

Meneghetti et al., [65] investigated the effect of building orientation on the tensile and fatigue parameters of Direct Metal Laser Sintered 300M steel (DMLS). Neither 0° nor 90° specimen building orientations resulted in variation in mechanical properties for either as-built or aged samples. The fatigue strength of specimens orientated at 0^{o} was found to be low.

Jyoti Suryawanshi et al. [66] also studied the tensile, fatigue crack growth and fracture properties of AM 300M steel processed through SLM. After aging, both conventional and SLM M300 showed similar fatigue crack growth characteristics. Tarun Bhardwaj et al. [67] studied the effect of directional and cross-directional scanning of powder bed on surface finish, density, mechanical properties and texture of AM 300M samples processed through direct metal laser sintering (DMLS). With cross-directional scanning strategy, better surface finish and densification were obtained in samples. Due to transformation of crystallographic texture into weaker ones and heat flux rotation, a preferred growth of columnar grains followed by epitaxial formation was seen in both the directions of cross-directional strategy. This resulted in higher compressive residual stresses and decrease in anisotropy. The mechanical properties of DMLSed samples were found to be in the range of wrought maraging steel 300.

Yi Yao et. al. [68] investigated the effect of build orientation on microstructure and anisotropy in mechanical properties. Weak texture was observed in as-built (AB) samples due to randomly oriented grains. The XY-oriented sample showed better strength properties than Z-built samples and their corresponding fractographs of tensile tested samples are shown in Fig.1.12. The horizontal fractures surfaces (b, c), depict microvoids with dimples, whereas the vertical samples' fracture surface (d, e), comparatively large voids with ductile fractures. The as-built microstructure exhibited two different morphologies i.e., equiaxed and columnar structure.

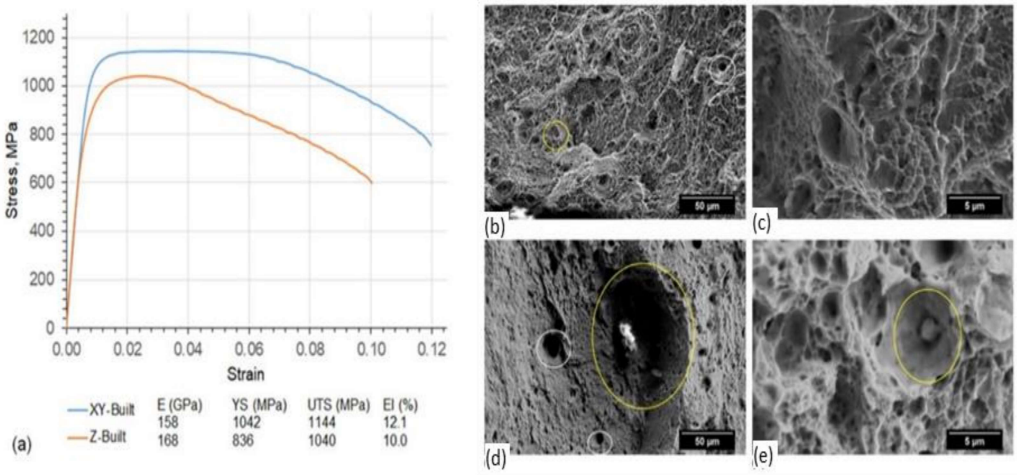

Fig. 1.12 (a) Stress-strain response of horizontal (XY-built) and vertical samples (Z-built), (b, c) fractographs of horizontal samples and (d, e) fractographs of vertical samples, both showing ductile fracture [68].

Y. Bai et al. [69] studied the influence of process parameters and evolution of mechanical properties of SLM processed maraging steel. Orthogonal technique to optimize process parameters was used. The energy density increases linearly with the increase in laser power. But when the laser power is higher than the certain value as shown in Fig.1.13, spatter and strong vaporization formed that resulted in decrease in relative density, even though scanning speed and scanning space were kept constant. It was observed that SLM processed steel showed relatively lower ductility and toughness than the values observed in wrought steel. After heat treatment, reduction in ductility was noticed.

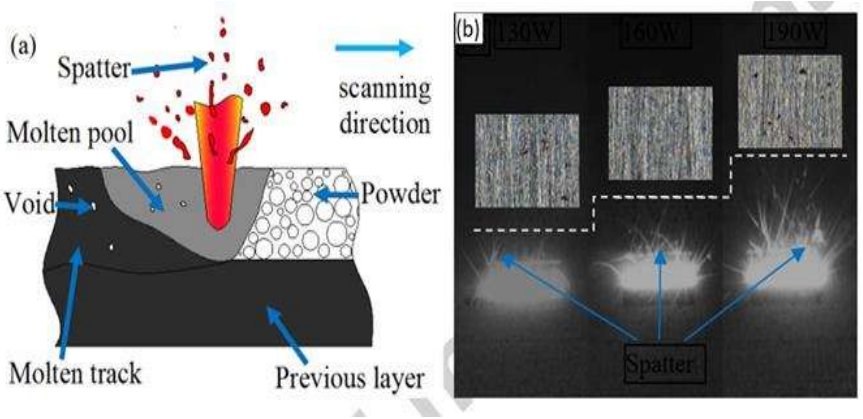

Fig.1.13 (a) Schematic view of high-power laser processing, showing spatter and vaporization (b) increase in spatter with laser power [69].

B. Mooney et. al. [70], investigated plastic anisotropy of additively manufactured maraging steel in 0^o, 45^o and 90^o build orientations. Considerable anisotropy was observed in as-built condition which was reduced after heat treatment. Heat treatment for 8h at 490°C was proposed to get optimum design strength ($R_{p0.2}$ >1900 MPa), whereas heat treatment for 8 h at 525°C aging treatment was suggested to obtain good isotropic compromise between design strength ($R_{p0.2}$ >1700 MPa) and ductility (A_f ~ 10%). The as-built and over aged specimen showed a higher level of planer anisotropy than those of under-aged and peak-aged specimens.

J. Mutua et. al., [71] optimized the process parameters and studied the effect of heat treatment on microstructure and mechanical properties. The process map of SLM maraging steel was designed. There is relatively large process window, where sound product with relatively higher density can be obtained, as shown in Fig.1.14(a). The quantity of austenite phase increased in aging treatment. Solution treatment/aging resulted in elimination of austenite phase and formation of intermetallic precipitates. The results indicated that the SLMed specimen with the build direction parallel to the loading direction had much lower elongation values than those with the build direction

perpendicular to the loading direction as shown in Fig.1.14(b). Aged samples showed maximum tensile strength of 2033 MPa while ductility decreased from 10.38% to 5.27%.

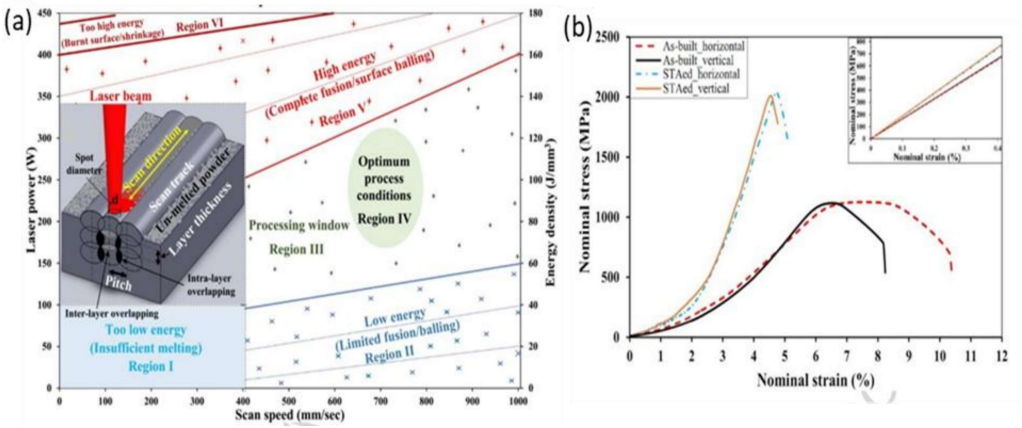

Fig. 1.14 (a) process parameter optimization widow for better part density (b) Stress-strain curves of horizontal and vertical samples in as-built and solution/ aging treated (STAed) conditions [71].

From the above literature, it can be seen that ductility is drastically reduced with increase in strength after heat treatment in maraging steels. Studies which focus on improving the ductility in AM maraging steels by suitable heat treatments are limited. Also, investigations which consider the effect of factors such as build orientation, residual stresses and density of parts along with detailed analysis of microstructural features obtained by optical, scanning and transmission electron microscopy which affect the mechanical properties of samples built in different orientations are very few. As mechanical properties of AM steels significantly vary in different orientations and also different from those of conventional steels, clear establishment of process-orientation-structure–property correlations are essential before such AM components are placed in service to prevent failures. The present work attempts to address these issues.

The present investigation aims at studying the effect of build orientation on microstructure and tensile behavior of M300 maraging steel processed by AM and effect of age hardening on microstructure and mechanical properties. Higher ageing temperature (520 ^{o}C) and time (5 hours) than that reported by most of the authors was

chosen for the present study which is close to working temperature of most of the extrusion dies used in industrial applications in order to study microstructural modifications of M300 maraging steel exposed to such high temperatures and their consequent effect on tensile behaviour.

1.9.2 LOW CYCLE FATIGUE (LCF) BEHAVIOR

Steels are the most common alloys and are widely used in almost every sector. The use of AM to process steel powder makes it more attractive and useful for mankind [72]. The weldability of steel greatly depends upon the carbon percentage, which is limited to approximately 0.2 wt.%C. Therefore, steel with minimal carbon is preferred in AM. Maraging steels are suitable for AM because of low carbon content and low reflectivity and good weldability. Additive Manufactured maraging steels are generally used in structural applications where static and dynamic loading bearing capacity are prime requirements [73].

Due to disparities in microstructure, defects and residual stresses, the mechanical properties of AM materials can vary substantially from those of conventionally manufactured materials. Therefore, it is essential to investigate the LCF behaviour of AM materials to assure their safe and reliable use in critical applications experiencing dynamic loading. Due to the presence of microstructural defects such as porosity, incomplete fusion and non-uniform grain structures, AM materials typically have a shorter LCF life than traditionally manufactured materials. Research investigations indicate that the LCF life of some AM materials can be 50% shorter than that of conventionally manufactured materials.

Under specific conditions, when the build direction is parallel/perpendicular with the loading direction, AM materials may result in different LCF properties [74]. Therefore,

it is essential to investigate the LCF behaviour of additive manufactured maraging steel in different orientations.

R. Baranco et. al. [75], studied the low cycle fatigue behaviour of SLMed maraging steel, with fully reversed (R= -1) loading conditions at various strain amplitudes (0.3%, 0.6%, 0.8%, 0.9% & 1.0%) with fixed strain rate (8×10^{-3} s^{-1}) and concluded that the steel showed strain softening throughout the entire life. It was also observed that as strain amplitude increased, the number of cycles to failure (N_f) decreased as per Table. 1.3. Fracture analysis showed a mixed mode of fracture, i.e., intergranular-trans granular.

Table 1.3 Summary of LCF results at varied strain amplitudes [75].

Specimen	Total Strain $\Delta\varepsilon/2$ (%)	Elastic Strain Amplitude, $\Delta\varepsilon_e/2$ (%)	Plastic Strain Amplitude, $\Delta\varepsilon_p/2$ (%)	Stress Amplitude, $\Delta\sigma/2$ (MPa)	Number of Cycles to Failure, N_f
D100	1.005	0.5975	0.4077	1005.0	33
D090	0.905	0.5891	0.3163	990.8	64
D080	0.807	0.5984	0.2087	1006.5	40
D060	0.609	0.5442	0.0644	915.3	129
D050	0.511	0.4764	0.0349	801.3	145
D040	0.411	0.4035	0.0080	678.7	1087
D035	0.362	0.3584	0.0034	602.8	2399
D030	0.304	0.3050	0.0012	512.9	5441

R. Nandhini et. al. [76], investigated fully reversed (R= -1) stress-controlled (high cycle fatigue) fatigue behaviour of AM 18Ni300 steel in X and Z directions in four conditions: as-printed (A), printed and machined (B), heat treated (C), and heat treated and machined (D). It was observed that printed sample in X direction, without any post-processing showed better fatigue strength than printed samples in Z direction. Similar results were

found in all post-processing conditions (B, C, D). It was also observed that heat treatment improved fatigue life but was not significant as machining.

R. Daniel et al. [77], studied the effect of defects on high cycle fatigue strength of AM maraging steel. Two batches of samples were used in fatigue testing. In the first batch, the sample axis was parallel to build direction (0^o) and in the second batch, the sample axis was perpendicular to the build direction (90^o). It was observed that (0^o) oriented samples exhibited fatigue strength, 45% to 60% higher than those oriented at 90^o.

The aforementioned research investigations were undertaken mostly under stress-controlled fatigue testing, with an emphasis on high-cycle fatigue regime. Comprehensive investigations on strain-controlled low-cycle fatigue research is not available in the open literature except those studied by Branco et. al. [75] which focused on studying the variation of strain amplitude on low cycle fatigue behaviour of maraging steel. There is no literature available that focuses on the effect of build orientation (0^o, 45^o and 90^o) and heat treatment on the LCF behaviour of maraging steel. The present work aims to study of LCF behaviour of maraging steel built in different orientations and the effect of heat treatment at fully reversible cycling, (R= -1), fixed strain rate (5×10^{-3} s^{-1}) and fixed strain amplitude (±0.5%).

1.9.3 WEAR BEHAVIOUR

Very limited research is available on the wear behaviour of additively manufactured materials, such as Al-Si alloy [78-80], Inconel 625 [81], titanium alloy [82, 83], stainless steels in general [84-86], and 316L stainless steel in particular [87].

Chaolin Tan et al. [61] found that wear rate of heat-treated specimens of maraging steel, decreased about 40-60% in comparison with that of the as-fabricated specimen and the

coefficient of friction values decreased after heat treatment. The observed average friction coefficients of as-fabricated, aging treated and solution-aging treated specimen were 0.62, 0.56, and 0.58 respectively. The variation of friction coefficient with time is shown in Fig. 1.15(a). The 3D morphology depicts the wear track after sliding wear as shown in Fig.1.15(b and c).

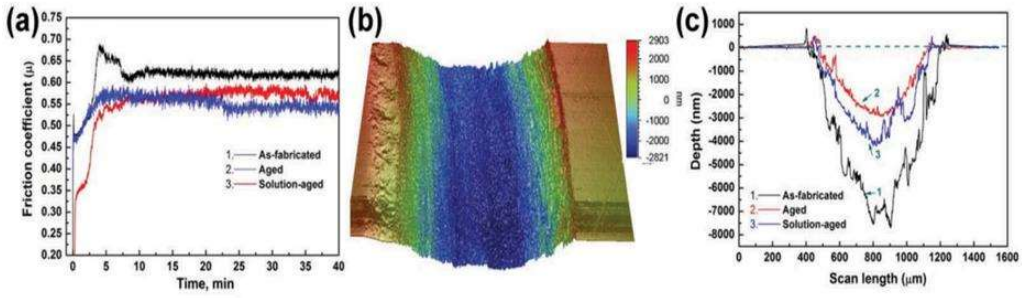

Fig. 1.15 (a) Variation of friction coefficient with time (b) 3D wear track morphology and (c) sectional line profiles of wear track of SLM specimens [61].

Daniel F. S. et al. [88] performed dry sliding pin on disc wear testing on maraging steel at 40N load and 0.4 m/s sliding velocity and observed from wear track analysis that average wear track depth for H13 steel with grain size of 215 μm was more than that of 18Ni300 maraging steel of 35 μm grain size. The 18Ni300 steel had grinding scratches, indicating abrasion wear mechanism while abrasive fatigue wear was more pronounced for the H13 Steel.

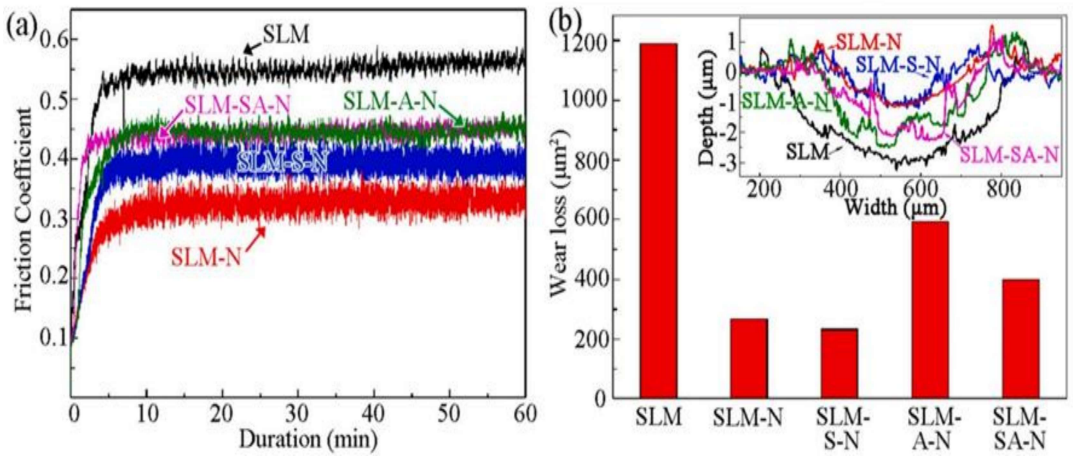

Fig. 1.16 The friction coefficients (a) and wear losses (b) in the tribological tests of as fabricated sample and nitrided samples. The inserted image shows the depth profiles of wear tracks [89].

Hong et al. [89] used plasma nitriding to enhance wear resistance of SLM 18Ni300 maraging steel and observed that the sample prepared by simultaneous aging and nitriding showed thickest nitriding layers and exhibited best wear resistance. Compared to the as-fabricated (SLM) sample, all other nitrided samples exhibited lower friction coefficient [Fig.1.16(a)] and less wear loss. As shown in Fig.1.16(b), the wear tracks of selective laser-melted plus plasma nitride (SLM-N) and solution treated selectively laser-melted plus plasma nitride (SLM-S-N) samples are narrower than those of aging treated selectively laser-melted plus plasma nitride (SLM-A-N) and solution aging treated selectively laser melted plus plasma nitride (SLM-SA-N) samples which is consistent with the results of wear losses. The evident grooves in all wear tracks indicated that abrasive wear was the main wear mechanism for all the nitrided samples. Many smears, as the characteristics of adhesive wear, also occurred in the grooves of the worn samples.

Shuo Yin et al, [90] studied the effect of aging time and temperature on tribological properties of SLM maraging steel. It was found that under optimized aging conditions (490^{o}C for 3hr), SLM maraging steel had best wear resistance. Wear mechanism varied

from abrasion to adhesion, after aging. Over and under aging also resulted in the decrease of strength and wear-resistance performance of the SLM maraging steel as compared with the optimal aging conditions. The variation of the mechanical and tribological properties is primarily due to changes in phase compositions and microstructures of the SLM maraging steels. The coefficient of friction (COF) of the aged sample was found to be always lower than that of the as-fabricated sample during the entire sliding testing as shown in Fig.1.17. The aged sample had a much lower COF (0.586 ± 0.071) than the value of the as-fabricated sample (0.629 ± 0.061). The wear mechanism of the aged sample was found to be adhesion tribofilm.

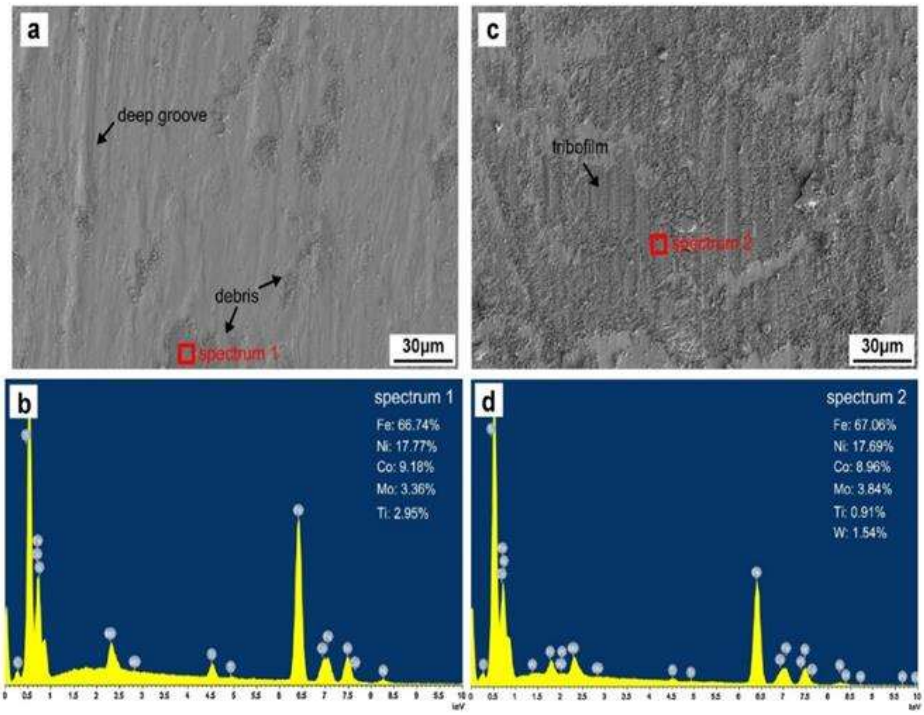

Fig. 1.17 Worn surfaces of the (a) as-fabricated and (b) aged SLM maraging steel (490 °C for 3 h) and (c, d) the corresponding EDX analysis. The atomic fraction of each element [90].

Ki Chang Bae et al. [91] studied the effect of build orientation, sliding velocity and heat treatment on SLM maraging steel by conducting ball on disc type wear tests. At low sliding speed of 25-100 mm/sec, wear rate of the as received sample was independent of

build orientation while at higher sliding speed of 500-1000 mm/sec, wear rate was found to be dependent on build direction. Abrasive wear was revealed to be the dominant wear mechanism at the relatively low sliding speed range of 25–100 mm/s. At the relatively high sliding speeds of 500 and 1000 mm/s, the plastic flow of the maraging steel was manifested near the worn surface and the delamination of the hardened area became the predominant wear mechanism. The samples with wear planes at 0^{o} and 45^{o} to the laser-scanning direction were designated as SD and 45SD, respectively, whereas the samples with a wear plane vertical to the building direction were designated as BD. The heat-treated (HT) SD, 45SD, and BD samples were marked as SD-HT, 45SD-HT, and BD-HT, respectively. Fig.1.18 illustrates the differences in the wear rates between the as-built and HT samples under the wear loads of 20 and 100 N and sliding speeds of 25–1000 mm/s.

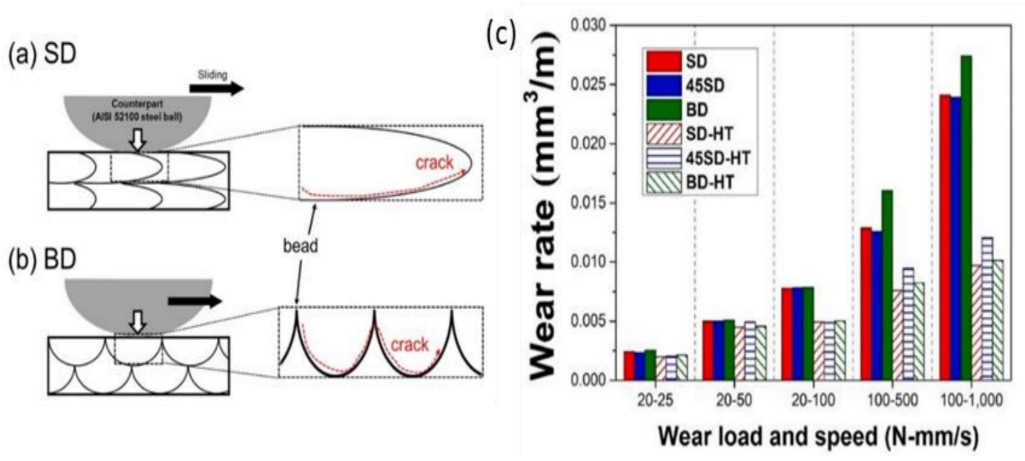

Fig. 1.18 Schematic diagram of the cross-section of wear tracks of (a) SD (b) BD for inferring the bead direction and crack propagation in the specimen and (c) comparison of wear rates after the wear testing with a total wear distance of 90 m under various wear loads and speeds [91].

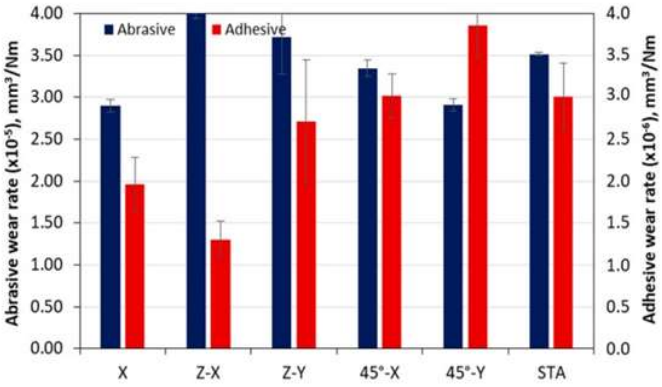

Fig.1.19 Effect of build direction, heat treatment and sliding orientation on the wear resistance of LPBF maraging steel [92].

B. Padgornik et al. [92] investigated dependence of wear resistance of SLM maraging steel on build direction and heat treatment and found the best combination of high adhesion and abrasion wear resistance for the horizontal build direction. By changing the printing direction and performing wear testing in the vertical plane, the wear rates were increased by more than 30% to about 3.9×10^{-5} mm^3/Nm. The orientation of the layers played a role as shown in Fig.1.19. The effect of the build and testing direction had little influence when the specimens were subjected to solution treatment and aging, with the wear rates observed are found to be between values for the vertical and horizontal build directions (~3.5×10^{-5} mm^3/Nm). Coefficient of friction was found to be independent of the build and/or sliding direction, as well as the heat treatment of the LPBF maraging steel.

1.9.4 EROSION BEHAVIOUR

Many critical parts such as rocket casings, pipes, bends and valves used in material transportation, automotive, aerospace and tool industries are now manufactured by additive manufacturing. These parts can be exposed to different streams of particles in different environments during their applications. Systematic experimental investigations

are very important to analyze the particle erosion behaviour of additive manufactured materials in general and steels in particular. Very limited studies are available on erosion behavior of additive manufactured alloys at present. Particle erosion study of additive manufactured material i.e., 316L stainless steel was recently reported.

Z. Azakli et. al., [93], studied the particle erosion behaviour of additive manufactured 316 L stainless steel, at different impingement angles at particle speed of 140 m/s, built with the variation of laser scanning speed. To examine the effect of process parameters on erosion, the samples were prepared at different laser scanning speeds. The sample were labelled as SLM#600, SLM#1000, SLM#1400, SLM#1800, the numbers indicating scanning speeds. The study showed mass loss behaviour of SLM samples showed a decrease in erosion rate of about 25-30% compared to that of forged 316L at all impact angles. SLMed sample built with different laser scan speeds had similar mass loss behaviour at all impingement angles except for 30^{o}. The reason for less erosion rate at higher angle of impingement is given as follows: As the impingement angle gets larger, the interactions between incoming and rebounding particles take place which decrease the kinetic energy of the incoming particle accordingly. The result is shown in Fig. 1.20.

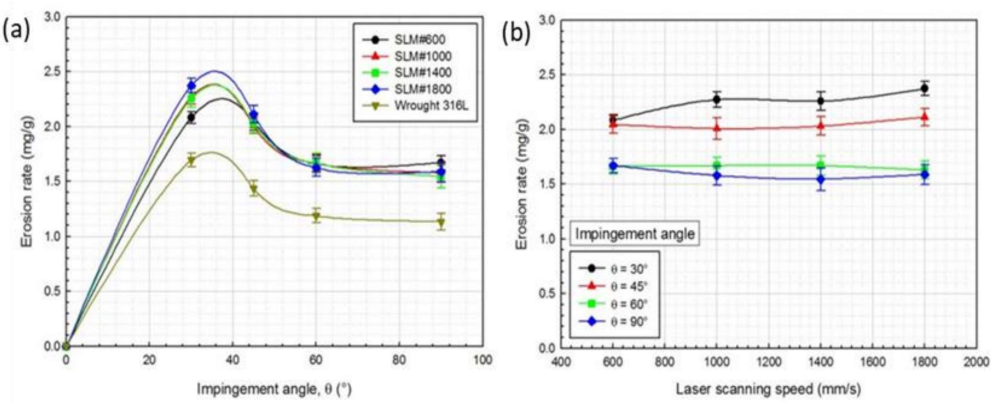

Fig.1.20 Variations of erosion rate with: (a) impingement angle and (b) laser scanning speed [93].

There is no literature available on the combined effect of build orientation and heat treatment on wear and erosion behaviour of maraging steel. In the present work, maraging steel plates were manufactured in 0^o, 45^o and 90^o orientations using SLM technology. The specimens were subjected to heat-treatment. Wear as well as erosion behavior was studied in the as built and also in heat-treated conditions. Realizing the importance of industrial applications of AM maraging steel, comprehensive performance of the SLM-produced specimens was taken up and compared with the performance of the traditionally fabricated (cast and hot rolled) maraging steel.

1.9.5 CORROSION BEHAVIOUR

In recent years, studies on the microstructure and corrosion behaviour of the components of metals and alloys, prepared by additive manufacturing (AM) have garnered widespread attention. Very limited research is available on the corrosion behaviour of additively manufactured steels, namely 316 L austenitic stainless steels [94], 17–4 PH [95] and 15–5 PH steels [96, 97], and maraging steels [98-100]. The majority of these investigations have focused on studying the influence of process parameters and heat treatments on microstructure, texturing, tensile, fatigue and wear attributes.

Fernandes et al. [101] investigated fatigue crack formation in L-PBF (Laser powder bed fusion) maraging steel, processed at different deposition planes (0^o, 45^o and 90^o), in saline corrosive environment and found that the amount of martensite (columnar grains) formed had a direct effect on corrosion rate of the different samples. The effect of saline media on fatigue crack growth was not seen to be significant. Fig.1.21 shows the potentiodynamic polarization curves for each deposition angle. The corrosion current density showed the following values: $\beta = 0^o$ ($i_{corr} = 3.571 \times 10^{-6}$ A/cm^2) > $\beta = 45^o$ ($i_{corr} = 5.334 \times 10^{-6}$ A/cm^2) > $\beta = 90^o$ ($i_{corr} = 7.771 \times 10^{-6}$ A/cm^2). The corrosion current density was highest in the sample produced with the deposition angle, $\beta = 90^\circ$, showing lowest

saline corrosion resistance. From these results, it can be concluded that the samples that had the highest amount of columnar grains showed a superior corrosion/oxidation resistance, which can induce a higher level of crack closure phenomena.

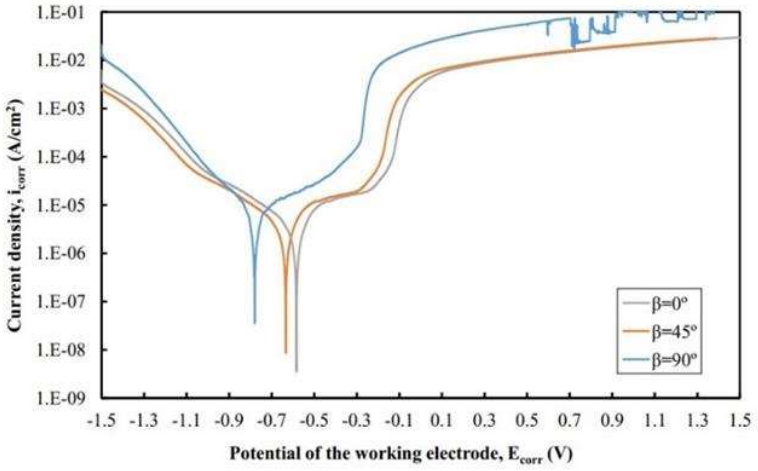

Fig.1.21 Potentiodynamic polarization curve [101].

Anoop et al. [102] examined stress corrosion cracking (SCC) of additively produced maraging steel in 3.5% NaCl. It was demonstrated that the hot isostatic pressing (HIP) treatment enhanced pitting corrosion resistance because of the austenite phase and the removal of defects such as pores as shown in Fig. 1.22 (a and b). Severe localized corrosion was seen for the STA sample, while the HIP-STA had revealed only few pits. EIS measurements were taken to analyze the corrosion behaviour and found that observed impedance values were higher for the HIP-STA samples compared to STA. The stress-strain curves of the SLM-processed M300 steel specimens obtained in air and 3.5% NaCl solution are shown in Fig.1.22(c). STA specimen failed in the elastic regime with significant loss in values of percentage elongation. Compared to STA samples, the reduction in elongation was less for the HIP-STA samples and the obtained SCC index value was found to be 0.88.

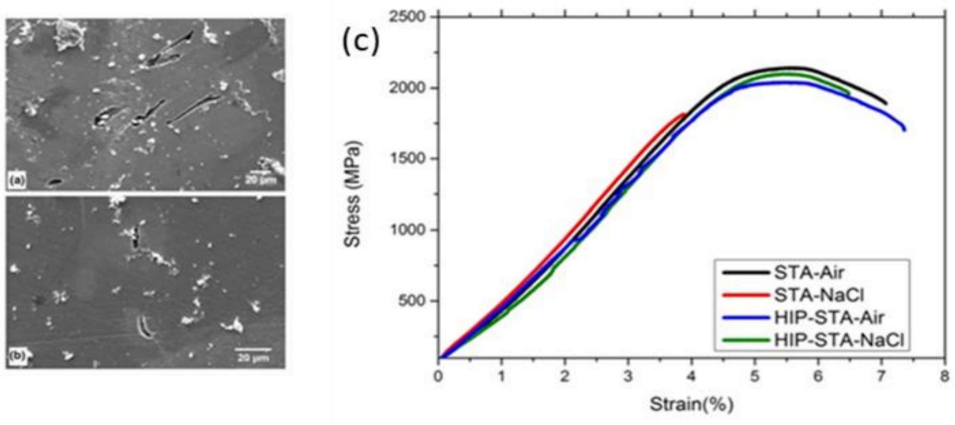

Fig. 1.22 Corrosion morphology of SLM-processed M300 samples and HIPed samples (a) STA (b) HIP-STA conditions and (c) stress vs strain plots for SLM-processed M300 maraging steel [102].

T Simson et al. [103] examined the corrosion behaviour of the 18Ni300 maraging steel and found that L-PBF samples were prone to pores and oxides, which affect the corrosion behaviour. According to the post-processes used such as milled, turned, sandblasted, as-build, grinded and laser treated, different corrosion parameters were analysed. The current density as a value for the corrosion rate I_{corr} – varying between 0.38 ~ 0.70 mA/cm² – does not show any significant influence due to change in the surface roughness. The additives samples were compared with conventional samples and it was observed that the manufacturing methods have no measurable effect and showed similar corrosion behaviour. The effect of heat treatment was also observed and it was found that the corrosion resistance of age-hardened samples was lower than that of solution-annealed samples. The lower corrosion resistance of the age-hardened specimen was due to galvanic effect. For the solution annealed samples, the corrosion current densities were in a range of I_{corr} = 0.38 ~ 0.7 mA/cm². The corrosion current densities of aged samples were, approximately twice as high of solution treated samples.

Rajesh et al. [104] compared the corrosion and wear behaviour of the DMLS (Direct Metal Laser Sintering) developed maraging steel and 316L steel and observed that

maraging steel exhibited better wear and corrosion resistance than 316L stainless steel. E_{corr} and I_{corr} values were less for stainless steel 316 L as compared to maraging steel.

Khan et al. [105] examined the effect of ageing and surface drag finishing post-processing treatments on corrosion behaviour of the SLM maraging steel and observed that after heat treatments, corrosion rate of the SLM maraging steel was increased. Different notations of samples were used in the experiment such as C00: no aging and no drag finishing, C01: no aging and drag finished, C10: aging and no drag finished sample, C11: both aging and drag finishing performed samples. Aging was performed at 490^{o}C for 6 hours. The electrochemical testing was carried out for 60 minutes at a scan rate of 0.5 mV/s in 3.5 % NaCl solution. Both aging and drag-finishing were found to be deleterious on the corrosion performance of the selectively laser melted steel, as shown in Fig.1.23. It was also observed that the drag-finishing process was found to aggravate the corrosion reaction more than the heat-treatment due to the formation of the cracks in the surface layer.

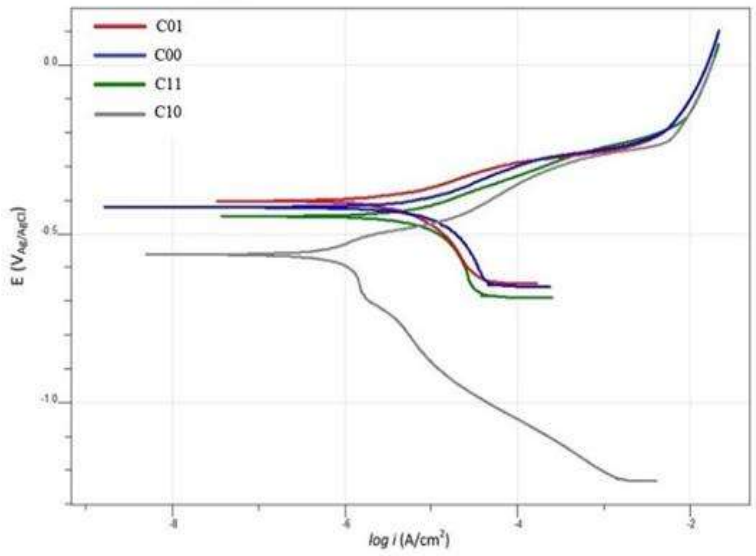

Fig. 1.23 Potentiodynamic polarization curves of the as built, heat-treated, and drag finishing samples [105].

Zhao et al. [106] investigated the influence of pore defects and different heat treatments on corrosion and mechanical properties of the SLM (Selective Laser Melting) M300 steel. The steel was solution treated at 820°C for 1 h, air-cooled and aged at 480°C for 2 hours (HT1) and 5 hours (HT2). It was observed that corrosion resistance was inversely proportional to pore size and the depth of pits and decreased with increase in the aging time due to coarsening of Ni_3Mo which caused shrinkage of surrounding pores.

Ozer et al. [107] examined the effect of solution treatment at 940°C for 2h and aging at 490°C for 6h on the microstructure, mechanical properties and corrosion resistance of the DMLS fabricated maraging steel. It was observed that due to change in microstructure, resulting from the heat treatment, there was decrease in corrosion resistance of the AM material and increase in strength parameters.

Ansell et al. [108] investigated mechanical properties of the SLM maraging steel in vertical (V), 45° and horizontal (H) samples in the as-built and heat treated (490°C/6h, 600°C/6h and 900°C/45 minutes) conditions, after exposing the tensile samples in simulated marine environment for 500 h. In as-built conditions, 45° and H samples showed higher tensile strength than strengths by V samples. All heat-treated samples showed reduction in strength parameters.

From above, one can infer that limited studies are available that solely focus on the effect of build orientation on corrosion behaviour of SLM maraging steel and comparison of the behavior with that of conventionally manufactured maraging steel. The present work was planned to study the effect of build orientation at 0°, 45°, and 90°, both in the as-built and heat-treated conditions on corrosion behaviour of AM maraging steel. The corrosion study was carried out in 3.5% NaCl solution, using potentiodynamic polarization and

Electrochemical Impedance Spectroscopy (EIS) and comparison was made with corrosion behaviour of conventionally manufactured steel.

1.10 SCOPE OF THE PRESENT WORK

Though AM has gained importance in biomedical and functional applications, the potential of

manufacturing AM structural parts has not yet fully explored. The main challenge is uncertainty in mechanical properties due to microstructural inhomogeneities and non-uniform

distribution of defects. Process parameters such as scan speed, laser power, layer thickness hatch spacing and thermal history in AM also affect the microstructural details and consequent mechanical behaviour. Even at the optimized process parameters, change in build parameters such as build orientation causes variation in microstructure and anisotropy in mechanical properties. Studies on optimizing process, microstructure, properties and performance of AM materials have therefore received major attention of researchers worldwide during last few years.

Maraging steels are group of high strength steels with low carbon content and contain Ni, Co, Mo and Ti as alloying element and can attain ultrahigh strength levels due to precipitation of intermetallic compounds during ageing treatment of martensite. Maraging steels have a wide range of aerospace applications such as landing gears of aircraft, missile casings, aircraft forgings, bearings, high power transmission shafts, fan shafts in commercial jet engines in addition to tooling and dies. In many of these applications, the steels are subjected to various kinds of stresses such as uniaxial, cyclic and/or thermal stresses. As mechanical properties of AM steels are significantly different from those of conventional steels, clear establishment of process-structure–property

correlations are essential before such AM components are placed in service to prevent failures.

The present work is therefore focused to study the effect of build orientation and heat treatment on the microstructure, tensile behaviour, low cycle fatigue behaviour, wear, erosion behaviour and corrosion behaviour of additively manufactured maraging steel. The findings can be utilized to improve the quality and reliability of additively manufactured maraging steel components in various applications. The present research can also play a crucial role in exploring new applications of additively manufactured parts in various industries. Overall, the findings of the present study can contribute significantly to the advancement of additive manufacturing technology in various sectors.

1.11 MOTIVATION FOR THE PRESENT WORK

Additive manufactured parts are exposed to different environments and loading such as static and dynamic loading during their applications. The direction and position of application of loading may vary as per usage of the parts. Maraging steels have a wide range of aerospace

applications such as landing gears of aircraft, missile casings, aircraft forgings, bearings, high power transmission shafts, fan shafts in commercial jet engines in addition to tooling and dies. In many of these applications, the steels are subjected to various kinds of stresses such as uniaxial, cyclic and/or thermal stresses. The applied load acting on components may be static and/or dynamic in nature and loading direction may also vary. Most interestingly, if the parts are manufactured by additive manufacturing, they contain layers and interlayer regions, and these regions are more prone to generation of defects as per orientation of the loading axis with the layer orientation of the part. A 3D model of a spherical ball processed by additive manufacturing in which layers can be seen

parallel to the build platform is presented in Fig.1.24(a) for better clarity and understanding.

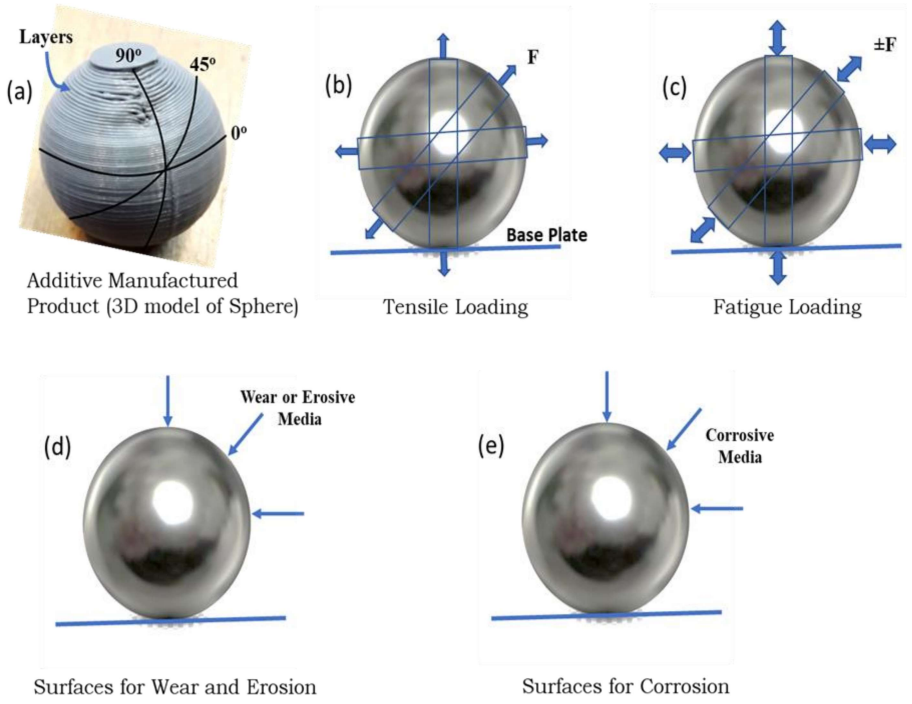

Fig. 1.24 (a) Additive manufactured 3D model of a sphere: (b) Tensile loading (c) Fatigue loading (d) surfaces for wear and erosion and (d) surfaces for corrosion, with respect to layer orientation.

Three orientations are considered: (i) the static/dynamic loads are applied along the layers (both layers and loading axis are parallel, 0^o orientation), (ii) transverse to the layers (both layers and loading axis are perpendicular to each other, 90^o orientation) and (iii) diagonally to the layers (both layers and loading axis are 45^o to each other, 45^o orientation) as shown in Figs.1.24. (b and c). If these parts are subjected to tensile and fatigue loading, tensile and fatigue behavior would be different and are dependent on the orientation relation between the loading axis and the layers. Similarly, if AM parts are exposed to the surrounding environment, where wear and erosion properties are required, then on the basis of parts exposed to the wear and erosive media [Fig. 1.24(d)], the material may behave differently depending on the orientation of layers. So, the wear and

erosion properties need to be analyzed with respect to the build orientation. Similarly, the corrosion behaviour depends on orientation of layers exposed to corrosive media [Fig. 1.24(e))] which is another important aspect to be explored in this investigation.

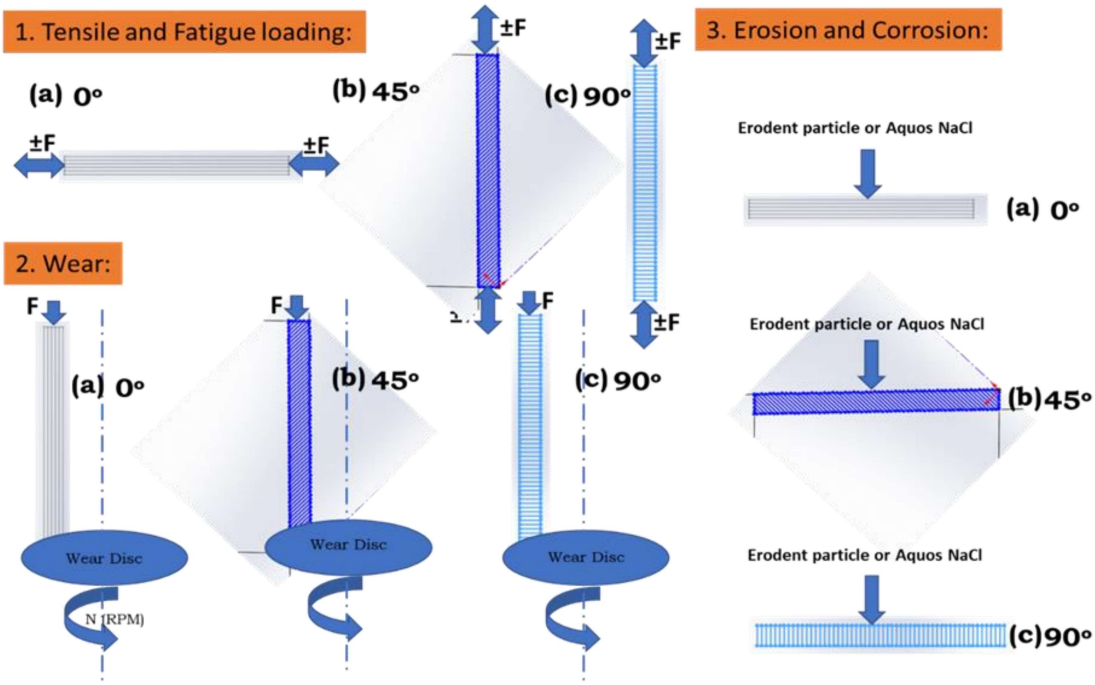

Fig. 1.25 Schematic presentation of samples built in 0°, 45°, and 90° orientations to the base plate.

To conduct the tensile, fatigue, wear, erosion, and corrosion studies, specimens of the required geometry will be processed by PBF-LB and machined to the required dimensions. To get the desired samples for tensile, wear, erosion, and corrosion and for fatigue samples in 0°, 45°, and 90° orientations, plates and rods of given dimensions were printed by PBF-LB. The schematic presentation of the samples in 0°, 45°, and 90° layers with respect to the loading axis and wear, erosion, and corrosion media is given in Fig. 1.25(1, 2, 3).

1.12 OBJECTIVES OF THE PRESENT INVESTIGATION

The objectives of the present investigation are as follows:

- To process maraging steel powder in 0^o, 45^o and 90^o build orientations by Powder Bed Fusion using Laser Beam (PBF-LB) and conduct post-heat treatment.
- To investigate the tensile behaviour of maraging steel processed by PBF-LB in 0^o, 45^o and 90^o build orientations and compare with the behaviour of conventionally manufactured maraging steel.
- To study low cycle fatigue behaviour of PBF-LB maraging steel processed in 0^o, 45^o and 90^o build orientations and to explore the effect of heat treatment on fatigue behaviour.
- To conduct wear and erosion testing of maraging steel samples processed by PBF-LB in 0^o, 45^o and 90^o build orientations and also subjected to heat treatment and analyze the factors responsible for good wear and erosion resistance.
- To investigate the corrosion behaviour of maraging steel samples processed in 0^o, 45^o and 90^o orientations by PBF-LB to find out best possible orientation for good corrosion resistance and assess the suitability of post heat treatment in improving corrosion behaviour.